



Published in final edited form as:

J Invest Dermatol. 2014 May ; 134(5): 1446–1455. doi:10.1038/jid.2013.532.

Ganglioside GM3 depletion reverses impaired wound healing in diabetic mice by activating IGF-1 and insulin receptors

Xiao-Qi Wang, Sarah Lee, Heather Wilson, Mark Seeger, Hristo Jordanov, Nandita Gatla, Adam Whittington, Daniel Bach, Jian-yun Lu, and Amy S Paller

Department of Dermatology, Northwestern University Feinberg School of Medicine, Chicago, IL

Abstract

Background—Ganglioside GM3 mediates adipocyte insulin resistance, but the role of GM3 in diabetic wound healing, a major cause of morbidity, is unclear.

Purpose—Determine whether GM3 depletion promotes diabetic wound healing and directly activates keratinocyte insulin pathway signaling.

Results—GM3 synthase (GM3S) expression is increased in human diabetic foot skin, ob/ob and diet-induced obese diabetic mouse skin, and mouse keratinocytes exposed to increased glucose. GM3S knockout in diet-induced obese mice prevents the diabetic wound healing defect. Keratinocyte proliferation, migration, and activation of insulin receptor (IR) and insulin growth factor-1 receptor (IGF-1R) are suppressed by excess glucose in wild type cells, but increased in GM3S^{-/-} keratinocytes with supplemental glucose. Co-immunoprecipitation of IR, IR substrate-1 (IRS-1), and IGF-1R, and increased IRS-1 and Akt phosphorylation accompany receptor activation. GM3 supplementation or inhibition of IGF-1R or PI3K reverses the increased migration of GM3S^{-/-} keratinocytes, whereas IR knockdown only partially suppresses migration.

Conclusions—Cutaneous GM3 accumulation may participate in the impaired wound healing of diet-induced diabetes by suppressing keratinocyte insulin/IGF-1 axis signaling. Strategies to deplete GM3S/GM3 may improve diabetic wound healing.

Keywords

Wound healing; keratinocyte; diabetes; glucose; migration; insulin receptor; insulin-like growth factor receptor; insulin receptor substrate-1 (IRS-1); Akt

INTRODUCTION

Chronic cutaneous ulcerations affects 15% of individuals with type 2 diabetes (Reiber *et al.*, 1998), often leading to amputation. The poor wound healing in diabetes has been linked to impaired insulin receptor (IR)/insulin-like growth factor-1 receptor (IGF-1R) signaling,

Users may view, print, copy, and download text and data-mine the content in such documents, for the purposes of academic research, subject always to the full Conditions of use:http://www.nature.com/authors/editorial_policies/license.html#terms

Correspondence: Amy S. Paller, MS, MD, Department of Dermatology, 676 N. St. Clair, Suite 1600, Chicago, IL 60611, Telephone: 312-695-3721, Fax: 312-695-0664, apaller@northwestern.edu.

Conflict of Interest: The authors have no conflict of interest to declare

accumulation of glycosylated end products, vasculopathy, neuropathy, and infection (Acosta *et al.*, 2008; Brem and Tomic-Canic, 2007; Christman *et al.*, 2011; Guo and Dipietro, 2010; Markuson *et al.*, 2009; Marston, 2006; Nouvong *et al.*, 2009; Peppas and Vlassara, 2005). While levels of glycosylated proteins are an accepted measure of glycemic control and their accumulation has been strongly linked to impaired acral wound healing in diabetics (Christman *et al.*, 2011; Markuson *et al.*, 2009), little is known about the role of increased glycolipids in diabetic wound healing.

Wound healing is a complex process that requires the activation, migration and proliferation of keratinocytes (KCs) to re-epithelialize the wound. Although skin is not a classical insulin target tissue, both insulin and IGF-1 have been shown to be potent stimulants of normal KC migration and proliferation through activation of IR and IGF-1R (Ando and Jensen, 1993; Li *et al.*, 2006). Indeed, studies in IR-null and IGF-1R-null mice have shown both IR and IGF-1R to be essential for normal keratinocyte physiology (Sadagurski *et al.*, 2006; Stachelscheid *et al.*, 2008). Nevertheless, the role of IR/IGF-1R signaling impairment in the compromised re-epithelialization of diabetic wounds is not well understood (Usui *et al.*, 2008).

Ganglioside GM3 has been suggested to play an intermediary role in the development of insulin resistance and diabetes. GM3, a sialylated membrane-based glycosphingolipid, and the enzyme that synthesizes it, GM3 synthase (*GM3S*; also called SAT-I/ ST3Gal-V), are increased in the kidneys, liver, adipose tissue and muscle of murine models of diabetes (Memon *et al.*, 1999; Tagami *et al.*, 2002; Zador *et al.*, 1993). Increased levels of gangliosides have been found in the serum of diabetic patients with microvascular complications (Hamed *et al.*, 2011), and *GM3S* expression is increased in the kidneys of diabetics with nephropathy (Wei *et al.*, 2011). Tumor necrosis factor alpha (TNF- α), which causes insulin resistance, increases *GM3S* and GM3 expression in canonical insulin target cells (adipocytes, myocytes and hepatocytes) (Memon *et al.*, 1999; Tagami *et al.*, 2002). Glucosylceramide synthase inhibitors deplete GM3 and reverse TNF- α -induced suppression of IRS-1 tyrosine phosphorylation in adipocytes (Aerts *et al.*, 2007; Tagami *et al.*, 2002). GM3 directly suppresses IR and IR substrate-1 (IRS-1) tyrosine phosphorylation in cultured adipocytes, decreasing glucose uptake (Tagami *et al.*, 2002). Knocking out *GM3S* in mice (Yamashita *et al.*, 2003) and treatment of diabetic mice or rats with glucosylceramide synthase inhibitors improves insulin sensitivity (Aerts *et al.*, 2007; Zhao *et al.*, 2009; Zhao *et al.*, 2007), ameliorates hepatic steatosis (Zhao *et al.*, 2009), and suppresses the development of diabetic renal hypertrophy (Zador *et al.*, 1993). The impact of gangliosides on IGF-1R activation has never been explored.

We have found increased expression of *GM3S* in the foot skin of human diabetics and of *GM3S* and GM3 in the skin of diabetic mice. Knocking out *GM3S* and depleting GM3 fully prevented the wound healing impairment of diet-induced obese (DIO) mice. Keratinocytes from *GM3S* knockout mice have activated IR and IGF-1R signaling and, as a result, accelerated migration and proliferation, particularly in the presence of excess glucose. We propose that *GM3S* and GM3 are key molecules in the development of insulin resistance and potential targets for therapies to improve diabetic wound healing.

RESULTS

Increased expression of GM3S in human and mouse diabetic skin

Human diabetic foot skin had a 4.1-fold increase in GM3S mRNA expression in comparison with age- and site-matched controls (Figure 1a). In the skin of two diabetic mouse models, *ob/ob* (leptin deficient) and C57BL/6 mice fed a high-fat diet (HFD) for 10 weeks (DIO), GM3S mRNA expression was increased by 4.2-fold and 3.0-fold, respectively (Figure 1b), and GM3 by 2.8- and 2.6-fold, respectively (Figure 1c). GM3 and GM3S were virtually undetectable in GM3S^{-/-} mouse skin.

GM3S depletion reverses the wound healing defect in DIO mice

To explore the effect of GM3S expression on wound healing *in vivo*, we compared the wound healing of GM3S^{-/-} and GM3^{+/+} littermate (WT) mice. Initially we confirmed the partial prevention of insulin resistance in GM3S^{-/-} mice fed a HFD for 10 wks as previously described (Yamashita *et al.*, 2003) (Supplemental Figure 1). GM3S^{-/-} HFD mice were as obese as their WT HFD littermates and showed high mean fasting glucose levels, but had normal fed insulin and glucose levels at 120 min after glucose challenge.

To more closely simulate human wound healing and reduce mouse skin contraction, we used a silicone splinted wound healing model (Galiano *et al.*, 2004), which allows healing primarily by re-epithelialization. Wound closure was visibly delayed in WT HFD mice by 5 days after wound initiation (Figure 2a and b), but wound closure in GM3S^{-/-} HFD and RD mice was similar. By only 3 days after wounding, the epidermal gap was greater in WT HFD vs. other mice, including GM3S^{-/-} HFD mice (Figure 2c, $p < 0.05$) and increased progressively ($p < 0.001$ for 5 and 7 days). Full epidermal closure required 14.1 days in WT HFD mice, but 7.4 days in GM3S^{-/-} HFD mice, and the rate was equal at all time points for GM3S^{-/-} HFD, GM3S^{-/-} RD, and WT RD mice (Figure 2c). Granulation tissue area was smaller in WT HFD wounds than in wounds from GM3S^{-/-} HFD mice (Figure 2d, $p < 0.05$ at 5 d and $p < 0.001$ at 7 d; Supplemental Figure 2), but the same in WT RD and GM3S^{-/-} HFD mouse wounds. WT HFD epidermis on day 3 wounds had fewer bromodeoxyuridine-positive (BrdU+) proliferating basal KCs ($p < 0.05$; Figure 2e) and a smaller migrational distance ($p < 0.05$; Figure 2f) than other mouse epidermis. These studies suggest that the accelerated wound healing *in vivo*, at least in part, is related to the observed increase in both keratinocyte proliferation and migration. Immunohistochemical analyses show that GM3S knockout reversed the deficit in p-IGF-1R staining seen in WT HFD mouse wound skin (Supplemental Figure 3).

Increased glucose exposure stimulates GM3S^{-/-} KC migration and proliferation

Pre-incubation of WT primary mouse KCs in 20 mM glucose for 72 h, traditionally used to simulate the hyperglycemic diabetic environment *in vitro* (Ingram *et al.*, 2008; Suzuki *et al.*, 2011), stopped migration in *in vitro* wounds (Figure 3a and b) and reduced cell proliferation (Figure 3c) (Lan *et al.*, 2008; Spravchikov *et al.*, 2001; Terashi *et al.*, 2005). GM3S^{-/-} cells migrated faster than WT cells by 24 h after wounding in normoglycemic conditions. In hyperglycemic medium, GM3S^{-/-} KCs closed wounds (Figure 3a and b) and proliferated faster (Figure 3c) than GM3S^{-/-} in normoglycemic medium or WT cells in normoglycemic

or hyperglycemic medium. Addition of supplemental GM3 eliminated the protective effect of GM3S depletion on glucose-induced suppression of migration and proliferation; no statistically significant difference was found when GM3S^{-/-} vs. WT KCs were treated with the combination of GM3 and high glucose at any time point (Figure 3a–c). In WT KCs, high glucose increased expression of GM3, as shown by immunofluorescence (Fig. 3d) and GM3S, as shown by Western blotting (Fig. 3e). Addition of the GM3 metabolic precursor lactosylceramide (LacCer), which is increased in GM3S knockout cells (Supplemental Figure 4a), did not affect WT KC proliferation (Supplemental Figure 4b) and decreased cell migration (Supplemental Figure 4c and d). These findings suggest that the increase in keratinocyte migration and proliferation, particularly with high glucose exposure, results directly from depletion of GM3 and not of increased LacCer.

GM3S depletion activates IR and IGF-1R signaling—GM3S depletion dramatically increased IR and IGF-1R phosphorylation and downstream activation, as shown in Figure 4a–e, but did not affect receptor expression (Supplemental Fig. 5). When cells were grown in normoglycemic medium (all panels at left of Figure 4), starved overnight, and stimulated with insulin, p-IR was 1.6-fold greater in GM3S^{-/-} KCs than in WT KCs (Figure 4a, top row and graph, lane 5 vs. 2; Supplemental Figure 5a, 2nd row). Under similar conditions, IGF-1 induced 7-fold more p-IR in GM3S^{-/-} KCs than in WT KCs (Figure 4a, top row, lane 6 vs. 3; Supplemental Figure 5a, left, 2nd row). In hyperglycemic medium for 72 h (all panels at right of Figure 4), p-IR responses to insulin and IGF-1 were reduced in WT cells, but increased in GM3S^{-/-} KCs (Figure 4a, lanes 7–12; Supplemental Figure 5a, right, 2nd row).

p-IGF-1R was 2.5-fold greater in normoglycemic medium after insulin stimulation and 1.9-fold greater after IGF-1 stimulation in GM3S-deficient vs. WT cells (Figure 4b, top row, lanes 5 vs. 2 and 6 vs. 3; Supplemental Figure 5a, bottom row). In hyperglycemic medium, p-IGF-1R was markedly reduced in WT KCs in the presence of either insulin (Figure 4b, lane 8 vs. 2) or IGF-1 (Figure 4b, lane 9 vs. 3). Despite exposure to high glucose, insulin-stimulated p-IGF-1R was maintained and IGF-1-stimulated p-IGF-1R was increased by 82% in GM3S^{-/-} KCs (Figure 4b, lanes 11 vs. 5 and 12 vs. 6, respectively). Even without growth factor stimulation, IGF-1R was activated in GM3S^{-/-} KCs and was further increased by 37% in the presence of supplemental glucose (Figure 4b, top row, lanes 10 vs. 4). Supplemental glucose did not affect IR or IGF-1R expression (Supplemental Figure 5b and c).

GM3S depletion increases the association of IR, IRS-1, and IGF-1R

In KCs, activation of IR or IGF-1R promotes their association with insulin receptor substrate 1 (IRS-1) (Sadagurski *et al.*, 2007), thereby activating IRS-1, phosphatidylinositol 3-kinase (PI3K), AKT, and other downstream pathway components. As expected, stimulation of WT KCs with insulin or IGF-1 led to the association of IRS-1 with IR (Figure 4c, 2nd row, lanes 3 and 4, respectively) and IGF-1R (Figure 4c, 5th row, lanes 3 and 4, respectively). In GM3S^{-/-} KCs, the insulin- and IGF-1-induced association of IRS-1 with IR (Figure 4c, 2nd row, lanes 6–7 vs. 3–4) was greater than that in WT KCs by 4-fold and 5-fold, respectively. The association of IRS-1 with IGF-1R was increased in GM3S^{-/-} vs. WT KCs by 8-fold

after insulin stimulation (Figure 4c, 5th row, lanes 6 vs. 3) and by 6-fold after IGF-1 stimulation (Figure 4c, 5th row, lanes 7 vs. 4). Even without growth factor stimulation, the associations in GM3S^{-/-} KCs of IRS-1 with IR (Figure 4c, row 2, lane 5 vs. 3) and of IRS-1 with IGF-1R (lane 5 vs. 4) were greater than in WT cells stimulated with growth factor. In WT KCs, IGF-1R co-immunoprecipitated with IR and vice versa (Figure 4c, rows 3 and 6), but only when stimulated with insulin (lane 3) or IGF-1 (lane 4). The association of IGF-1R with IR was increased in GM3S^{-/-} KCs vs. WT KCs after insulin stimulation by 2.3-fold (Figure 4c, row 3, lanes 6 vs. 3) and after IGF-1 stimulation by 5.7-fold (Figure 4c, row 3, lanes 7 vs. 4). In the complementary experiment, the association of IR with IGF-1R was also increased in GM3S^{-/-} KCs vs. WT KCs, particularly with IGF-1 stimulation (Figure 4c, row 6, lanes 6 vs. 3 and lanes 7 vs. 4).

Glucose supplementation to WT cells decreased IRS-1 co-immunoprecipitation with IR in the presence of ligands by approximately 60% (Figure 4c, row 2, lanes 10–11 vs. 3–4) and with IGF-1R by 92% (Figure 4c, row 5, lanes 10–11 vs. 3–4). In contrast, glucose supplementation to GM3S^{-/-} cells increased IRS-1 co-immunoprecipitation with IR or IGF-1R by up to 2.7-fold (Figure 4c, rows 2 and 5, lanes 12–14 vs. 5–7). Co-immunoprecipitation of IR with IGF-1R in ligand-stimulated WT cells was virtually eliminated by glucose supplementation (Figure 4c, rows 3 and 6, lanes 10–11 vs. 3–4), but was maintained or increased by up to 2-fold in GM3S^{-/-} cells (Figure 4c, rows 3 and 6, lanes 12–14 vs. 5–7).

GM3S depletion activates IRS-1 and downstream signaling

Increased glucose inhibited insulin- and IGF-1-induced p-IRS-1 in WT cells by 100% and 20%, respectively (Figure 4d, bottom row, lanes 10–11 vs. 3–4). GM3S depletion led to a 4-fold increase in p-IRS-1 (Figure 4d, bottom row, lanes 6–7 vs. 3–4), which more than doubled under hyperglycemic conditions (Figure 4d, bottom row, lanes 13–14 vs. 6–7). GM3S depletion increased ligand-induced p-AKT at Ser⁴⁷³ by approximately 4-fold in normoglycemic medium (Figure 4e, middle row, lanes 5–6 vs. 2–3). Supplemental glucose eliminated p-AKT in WT cells (Figure 4e, middle row, lanes 8–9 vs. 2–3), but increased p-AKT in GM3S^{-/-} cells by 7.3- and 2.5-fold with insulin and IGF-1 stimulation, respectively (Figure 4e, middle row, lanes 11–12 vs. 5–6). Even without growth factor stimulation, p-AKT was detectable in GM3S^{-/-} KCs and increased 4-fold in hyperglycemic medium (Figure 4e, middle row, lane 10 vs. 4). GM3S depletion and glucose exposure did not affect expression of IRS-1 (Figure 4d, top row; Supplemental Figure 5d) or AKT (Figure 4e, top row).

IGF-1R is critical for the accelerated migration of GM3S^{-/-} KCs

Finally, we addressed the relative importance of IR vs. IGF-1R activation in stimulating GM3S^{-/-} KC migration. Small molecule inhibitors of IR were non-specific and inhibited IGF-1R, whereas the IGF-1R inhibitor AG538 did not inhibit IR phosphorylation. As a result, we transiently transduced an IR shRNA lentivirus into WT and GM3S^{-/-} mouse KCs, which knocked down IR by 55% and reduced p-IR by 87% in comparison with untreated and control shRNA-transduced cells, but did not alter IGF-1R expression (Figure 5a) or phosphorylation. AG538, in contrast, suppressed IGF-1R activation by 95% without

affecting expression or phosphorylation of IR (Figure 5b). To be able to compare the impact of inhibitors on WT vs. GM3S^{-/-} cells in normal glucose vs. GM3S^{-/-} cells in high glucose, scratch assays were performed with all cell types and conditions in parallel. Treatment of WT cells with IR shRNA, AG538, or LY294002 (which inhibits downstream PI3K) reduced *in vitro* wound closure after 60 h by about 50%, while treatment with the combination of IR shRNA+AG538 decreased migration to the same extent as GM3 (50 μM), supplemental glucose, or IR sh/AG538 with or without GM3 or glucose (all 70%) (Figure 5c, Supplemental Figure 6). In contrast, IR shRNA reduced migration after 60 h of the GM3S^{-/-} KCs without extra glucose by only 26%, while AG538, the combination of IR shRNA +AG538, GM3, and LY294002 similarly reduced migration by approximately 56% (Figure 5d; Supplemental Figure 6). In the presence of supplemental glucose (G), GM3S^{-/-} KC migration was accelerated. As in GM3S^{-/-} KCs grown without high glucose, IR shRNA only reduced migration by 27%; however, AG538 alone, LY294002, AG538+IR shRNA, GM3, and the combination of AG538+IR shRNA+GM3 all reversed the stimulatory effect on migration of GM3S^{-/-} KCs in high glucose beginning 24 h after the scratch (and by 60–65% at 60 h). Treatment of GM3S^{-/-} KCs in high glucose with both inhibitors or GM3 suppressed migration to the same extent as WT KCs treatment with GM3 and AG538+IR shRNA (Figure 5e; Supplemental Figure 6). These data provide further evidence of a key role for activation of IGF-1R signaling in accelerated wound healing in GM3S^{-/-} HFD mice.

DISCUSSION

Despite intriguing evidence that GM3 is a key intermediary in the development of insulin resistance in canonical insulin target tissues, the effect of GM3 depletion on peripheral tissues and diabetic wound healing has never been explored. We now show that GM3S depletion fully reverses the impairment in wound healing in a DIO diabetic mouse model, despite mouse obesity and only partial improvement in systemic glucose homeostasis. In this model, increases in both migration and proliferation of KCs contribute to the accelerated healing (Seitz *et al.*, 2010). Furthermore, we have demonstrated a direct effect of GM3S depletion on KC motility and proliferation *in vitro* through activation of insulin/IGF-1 axis signaling.

This stimulatory effect of GM3S depletion on KC motility and proliferation is intensified when KCs are made “diabetic” through exposure to increased glucose, as opposed to the marked inhibition of WT KC migration and proliferation by supplemental glucose. In other studies, we have found that accumulation of GM3 through gene suppression of enzymes regulating GM3 metabolism suppresses KC migration and proliferation (unpublished data, ASP); coupled with the lack of stimulation of KC migration and proliferation by LacCer, the GM3S substrate, these data implicate depletion of GM3 itself as the cause of the stimulatory effects of GM3S knockdown. Furthermore, these observations suggest a central role for KC GM3 in the wound healing defect of obesity-related diabetes (see schematic, Supplemental Figure 6).

In ganglioside-depleted adipocytes, the resultant increase in insulin sensitivity has been linked to adipocyte IR activation (Kabayama *et al.*, 2005; Tagami *et al.*, 2002). We have

now shown that GM3 depletion increases IR sensitivity in KCs not only to insulin but also to IGF-1. Importantly, we have demonstrated that GM3 affects IGF-1R signaling, which to our knowledge is previously unreported. At least in KCs, the impact on IGF-1R appears to be more significant in controlling cell migration than the effect on IR. Indeed, IGF-1, which is produced by dermal fibroblasts, stimulates KC proliferation (Ando and Jensen, 1993; Haase *et al.*, 2003) and accelerates *in vitro* (Haase *et al.*, 2003) and *in vivo* (Jeschke *et al.*, 2004; Jyung *et al.*, 1994; Semenova *et al.*, 2008) wound healing. mIGF-1 transgenic mice have a hyperplastic epidermis and accelerated wound healing (Semenova *et al.*, 2008), while IGF-1R^{-/-} mice show skin hypotrophy and delayed wound healing (Liu *et al.*, 1993). Diabetic wounds are deficient in IGF-1 (Blakytyn *et al.*, 2000) and, as we have now demonstrated, decreased in IGF-1R activation. In other studies, we have also found decreased p-IGF-1R, p-IR, and pSer⁴⁷³-Akt expression by Western blotting in the wounds of WT HFD mice, but not GM3S^{-/-} HFD or WT RD mice (data not shown). The prevention of hyperglycemia-induced suppression of IR and IGF-1R signaling, migration, and proliferation by GM3S depletion, and its reversal when exogenous GM3 is added, further suggest that GM3 is a key mediator of insulin resistance.

Gangliosides are thought to impact signaling primarily at the membrane level through regulating interactions of lipid raft components (Sonnino and Prinetti, 2010). Although IR and IGF-1R localization in primary KC membranes is not defined, both receptors signal in caveolar lipid rafts in other cell types (Kabayama *et al.*, 2007; Romanelli *et al.*, 2009; Sekimoto *et al.*, 2012), and IGF-1R signaling requires caveolin-1 in keratinocyte-derived HaCaT cells (Salani *et al.*, 2010). In adipocytes, increases in membrane GM3 content by chronic exposure to low concentrations of TNF- α , prevents the localization of IR to caveolar domains (Kabayama *et al.*, 2005; Kabayama *et al.*, 2007; Sekimoto *et al.*, 2012). When GM3 content is reduced, IR accumulates in these lipid raft domains, associates to a greater extent with caveolin-1, and is activated (Kabayama *et al.*, 2005). Ganglioside depletion may similarly prevent IR, and possibly IGF-1R, from leaving caveolar domains in KCs, leading to increased receptor activation and downstream signaling.

MATERIALS & METHODS (see Supplemental Methods)

Mouse models, human diabetic skin, and cultured mouse keratinocytes

Human diabetic and age-matched volunteer control plantar foot skin was obtained after written Northwestern IRB-approved informed patient consent according to Declaration of Helsinki guidelines; adipose tissue was removed prior to analyses. Mouse studies were approved by Northwestern's Animal Care and Use Committee. Male GM3S^{-/-} mice (Yamashita *et al.*, 2003) and wildtype (WT) GM3S^{+/+} littermate mice were fed a regular (RD) or 42% high fat diet (HFD) for 10 weeks and throughout analyses. ob/ob mice were from Jackson Labs. Mouse KCs were isolated from GM3S^{-/-} or WT skin at 1 day of age (Hamill *et al.*, 2012) and were used at passages 2–3.

Glucose tolerance tests and insulin measurement

Glucose tolerance testing (GTT) and fed insulin measurements were performed after 10 wks on a RD or HFD and at least 1 wk before wounding studies.

Detection of GM3 and gene expression in skin and KCs

Total ganglioside was extracted (Wang *et al.*, 2001) from mouse skin. GM3 expression was determined by thin-layer chromatography immunostaining using anti-GM3 antibody with loading normalized to cell number and densitometry to quantify (DH2, Glycotech, Gaithersburg, MD) (Wang *et al.*, 2002); the same antibody was used with FITC secondary antibody to detect GM3 by immunofluorescence. Gene expression of mouse GM3S, IR, IGF-1R, and IRS-1 was assessed on extracted total RNA by qRT-PCR and of human foot skin GM3S by droplet digital PCR (ddPCR) (see Supplemental Table 1 and Methods).

In vivo wound healing analysis

5 mm wounds were made on each side of the dorsal midline to below the panniculus carnosus and a donut-shaped silicone splint with a 6 mm inner circle was adhered to the surrounding skin to prevent contracture (Galiano *et al.*, 2004). Wound closure was analyzed at days 3, 5, 7, and every 3 days until healed by standardized photography and digital imaging. Wounds were harvested on days 3, 5, and 7, and processed for histologic, immunohistochemical, and RNA expression studies. All histological analyses to determine epidermal gap and granulation tissue area and immunohistochemical studies were performed at Northwestern's Skin Disease Research Center.

In vitro proliferation and migration assays

To simulate hyperglycemia, mouse KC medium (8 mM glucose) was supplemented with 12 mM glucose (Sigma, St. Louis, MO) for 72 h. Proliferation (measured by Water Soluble Tetrazolium assay) and cell migration (by scratch assays in the presence of mitomycin C) (Wang *et al.*, 2003) were performed in: a) WT KCs pretreated for 72 h with LacCer (5 μ M, Matreya LLC, Pleasant Gap, PA) (Mu *et al.*, 2009); b) GM3S^{-/-} KCs pretreated for 48 h with GM3 (50 μ M, Matreya)(Paller *et al.*, 1993); c) GM3S^{-/-} and WT cells pretreated 24h with IGF-1R- specific inhibitor AG538 (4 μ M, CalBiochem, Billerica, CA) or PI3K inhibitor LY294002 (20 μ M, CalBioChem, Billerica, MA); or d) GM3S^{-/-} and WT cells transduced with IR sh RNA or its vector control (Santa Cruz, CA) for 72 h.

Immunoblotting and immunoprecipitation

Immunoblotting was performed (Wang *et al.*, 2003) to detect IR, IGF-1R, IRS-1, Akt, GM3S, p-IR, p-IGF-IR, p-IRS-1, p-Ser473 Akt, and PY-20. Primary mouse KCs were treated with or without supplemental glucose in complete medium for 72 h. Cells were then starved of growth supplements and stimulated with or without insulin (5 μ g/mL, Sigma) for 15 mins or IGF-1 (100 ng/mL, Prospect, East Brunswick, NJ) for 30 mins. Selected times represent maximal stimulation times for each growth factor based on preliminary studies with exposure times of 5, 15, 30 and 60 mins; each was performed 3–5 times. Immunoprecipitation of IR, IGF-1R and IRS-1 were performed as previously described (Wang *et al.*, 2007) with IgG as a negative control.

Statistical analysis

Statistical significance of mouse wound healing data was determined by ANOVA followed by Fisher's least significant difference post-hoc testing for individual comparisons; data at

each time point was expressed as means±S.E. Mouse skin qRT-PCR and thin-layer chromatography data, as well as BrdU tissue labeling data, were expressed as means ± S.D. *In vitro* KC results and analyses of mouse skin for GM3 and GM3S expression were analyzed by paired Student's t-test, and expressed as mean±S.D. $p < 0.05$ was considered significant.

Supplementary Material

Refer to Web version on PubMed Central for supplementary material.

Acknowledgments

We acknowledge Dr. Pedram Yazdan for directing the blind review of microscopic images and Dr. Mark Eskandari for providing the human diabetic foot skin. This work was supported by the National Institutes of Health Grants R01AR44619 and R21AR062898 (AP) and the Astellas Research Endowment (XW). This research utilized Core resources provided by the NIH-funded Northwestern University Skin Disease Research Center (NIAMS, P30AR057216). We acknowledge Drs. Robert Lavker and Vincent Cryns for their careful review of the final manuscript.

Abbreviations

BrdU	bromodeoxyuridine
DIO	diet-induced obesity
DM	diabetes mellitus
GM3S	GM3 synthase
HFD	high fat diet
IGF-1R	insulin-like growth factor receptor-1
IR	insulin receptor
IRS-1	insulin receptor substrate-1
KC	keratinocyte
PI3K	phosphatidylinositol-3 kinase
RD	regular diet
WT	wildtype

References

- Acosta JB, del Barco DG, Vera DC, Savigne W, Lopez-Saura P, Guillen Nieto G, et al. The pro-inflammatory environment in recalcitrant diabetic foot wounds. *Int Wound J*. 2008; 5:530–9. [PubMed: 19006574]
- Aerts JM, Ottenhoff R, Powlson AS, Grefhorst A, van Eijk M, Dubbelhuis PF, et al. Pharmacological inhibition of glucosylceramide synthase enhances insulin sensitivity. *Diabetes*. 2007; 56:1341–9. [PubMed: 17287460]
- Ando Y, Jensen PJ. Epidermal growth factor and insulin-like growth factor I enhance keratinocyte migration. *J Invest Dermatol*. 1993; 100:633–9. [PubMed: 8491986]

- Blakytyn R, Jude EB, Martin Gibson J, Boulton AJ, Ferguson MW. Lack of insulin-like growth factor 1 (IGF1) in the basal keratinocyte layer of diabetic skin and diabetic foot ulcers. *J Pathol.* 2000; 190:589–94. [PubMed: 10727985]
- Brem H, Tomic-Canic M. Cellular and molecular basis of wound healing in diabetes. *J Clin Invest.* 2007; 117:1219–22. [PubMed: 17476353]
- Christman AL, Selvin E, Margolis DJ, Lazarus GS, Garza LA. Hemoglobin A1c Predicts Healing Rate in Diabetic Wounds. *J Invest Dermatol.* 2011; 131:2121–7. [PubMed: 21697890]
- Galiano RD, Michaels J, Dobryansky M, Levine JP, Gurtner GC. Quantitative and reproducible murine model of excisional wound healing. *Wound Repair Regen.* 2004; 12:485–92. [PubMed: 15260814]
- Guo S, Dipietro LA. Factors affecting wound healing. *J Dent Res.* 2010; 89:219–29. [PubMed: 20139336]
- Haase I, Evans R, Pofahl R, Watt FM. Regulation of keratinocyte shape, migration and wound epithelialization by IGF-1- and EGF-dependent signalling pathways. *J Cell Sci.* 2003; 116:3227–38. [PubMed: 12829742]
- Hamed EA, Zakary MM, Abdelal RM, Abdel Moneim EM. Vasculopathy in type 2 diabetes mellitus: role of specific angiogenic modulators. *J Physiol Biochem.* 2011; 67:339–49. [PubMed: 21336648]
- Hamill KJ, Hopkinson SB, Hoover P, Todorovic V, Green KJ, Jones JC. Fibronectin expression determines skin cell motile behavior. *J Invest Dermatol.* 2012; 132:448–57. [PubMed: 21956124]
- Ingram DA, Lien IZ, Mead LE, Estes M, Prater DN, Derr-Yellin E, et al. In vitro hyperglycemia or a diabetic intrauterine environment reduces neonatal endothelial colony-forming cell numbers and function. *Diabetes.* 2008; 57:724–31. [PubMed: 18086900]
- Jeschke MG, Schubert T, Klein D. Exogenous liposomal IGF-I cDNA gene transfer leads to endogenous cellular and physiological responses in an acute wound. *Am J Physiol Regul Integr Comp Physiol.* 2004; 286:R958–66. [PubMed: 15068969]
- Jyung RW, Mustoe JA, Busby WH, Clemmons DR. Increased wound-breaking strength induced by insulin-like growth factor I in combination with insulin-like growth factor binding protein-1. *Surgery.* 1994; 115:233–9. [PubMed: 7508640]
- Kabayama K, Sato T, Kitamura F, Uemura S, Kang BW, Igarashi Y, et al. TNFalpha-induced insulin resistance in adipocytes as a membrane microdomain disorder: involvement of ganglioside GM3. *Glycobiology.* 2005; 15:21–9. [PubMed: 15306563]
- Kabayama K, Sato T, Saito K, Loberto N, Prinetti A, Sonnino S, et al. Dissociation of the insulin receptor and caveolin-1 complex by ganglioside GM3 in the state of insulin resistance. *Proc Natl Acad Sci U S A.* 2007; 104:13678–83. [PubMed: 17699617]
- Lan CC, Liu IH, Fang AH, Wen CH, Wu CS. Hyperglycaemic conditions decrease cultured keratinocyte mobility: implications for impaired wound healing in patients with diabetes. *Br J Dermatol.* 2008; 159:1103–15. [PubMed: 18717678]
- Li Y, Fan J, Chen M, Li W, Woodley DT. Transforming growth factor-alpha: a major human serum factor that promotes human keratinocyte migration. *J Invest Dermatol.* 2006; 126:2096–105. [PubMed: 16691197]
- Liu JP, Baker J, Perkins AS, Robertson EJ, Efstratiadis A. Mice carrying null mutations of the genes encoding insulin-like growth factor I (Igf-1) and type 1 IGF receptor (Igf1r). *Cell.* 1993; 75:59–72. [PubMed: 8402901]
- Markuson M, Hanson D, Anderson J, Langemo D, Hunter S, Thompson P, et al. The relationship between hemoglobin A(1c) values and healing time for lower extremity ulcers in individuals with diabetes. *Adv Skin Wound Care.* 2009; 22:365–72. [PubMed: 19638800]
- Marston WA. Risk factors associated with healing chronic diabetic foot ulcers: the importance of hyperglycemia. *Ostomy Wound Manage.* 2006; 52:26–8. 30. 2 passim. [PubMed: 16567857]
- Memon RA, Holleran WM, Uchida Y, Moser AH, Ichikawa S, Hirabayashi Y, et al. Regulation of glycosphingolipid metabolism in liver during the acute phase response. *J Biol Chem.* 1999; 274:19707–13. [PubMed: 10391911]

- Mu H, Wang X, Wang H, Lin P, Yao Q, Chen C. Lactosylceramide promotes cell migration and proliferation through activation of ERK1/2 in human aortic smooth muscle cells. *Am J Physiol Heart Circ Physiol*. 2009; 297:H400–8. [PubMed: 19465542]
- Nouvong A, Hoogwerf B, Mohler E, Davis B, Tajaddini A, Medenilla E. Evaluation of diabetic foot ulcer healing with hyperspectral imaging of oxyhemoglobin and deoxyhemoglobin. *Diabetes Care*. 2009; 32:2056–61. [PubMed: 19641161]
- Paller AS, Arnsmeier SL, Alvarez-Franco M, Bremer EG. Ganglioside GM3 inhibits the proliferation of cultured keratinocytes. *J Invest Dermatol*. 1993; 100:841–5. [PubMed: 8496625]
- Peppas M, Vlassara H. Advanced glycation end products and diabetic complications: a general overview. *Hormones (Athens)*. 2005; 4:28–37. [PubMed: 16574629]
- Reiber GE, Lipsky BA, Gibbons GW. The burden of diabetic foot ulcers. *Am J Surg*. 1998; 176:5S–10S. [PubMed: 9777967]
- Romanelli RJ, Mahajan KR, Fulmer CG, Wood TL. Insulin-like growth factor-I-stimulated Akt phosphorylation and oligodendrocyte progenitor cell survival require cholesterol-enriched membranes. *J Neurosci Res*. 2009; 87:3369–77. [PubMed: 19382214]
- Sadagurski M, Nofech-Mozes S, Weingarten G, White MF, Kadowaki T, Wertheimer E. Insulin receptor substrate 1 (IRS-1) plays a unique role in normal epidermal physiology. *J Cell Physiol*. 2007; 213:519–27. [PubMed: 17508357]
- Sadagurski M, Yakar S, Weingarten G, Holzenberger M, Rhodes CJ, Breitkreutz D, et al. Insulin-like growth factor 1 receptor signaling regulates skin development and inhibits skin keratinocyte differentiation. *Mol Cell Biol*. 2006; 26:2675–87. [PubMed: 16537911]
- Salani B, Passalacqua M, Maffioli S, Briatore L, Hamoudane M, Contini P, et al. IGF-IR internalizes with Caveolin-1 and PTRF/Cavin in HaCat cells. *PLoS One*. 2010; 5:e14157. [PubMed: 21152401]
- Seitz O, Schurmann C, Hermes N, Muller E, Pfeilschifter J, Frank S, et al. Wound healing in mice with high-fat diet- or ob gene-induced diabetes-obesity syndromes: a comparative study. *Exp Diabetes Res*. 2010; 2010:476969. [PubMed: 21318183]
- Sekimoto J, Kabayama K, Gohara K, Inokuchi J. Dissociation of the insulin receptor from caveolae during TNF α -induced insulin resistance and its recovery by D-PDMP. *FEBS Lett*. 2012; 586:191–5. [PubMed: 22200571]
- Semenova E, Koegel H, Hasse S, Klatte JE, Slonimsky E, Bilbao D, et al. Overexpression of mIGF-1 in keratinocytes improves wound healing and accelerates hair follicle formation and cycling in mice. *Am J Pathol*. 2008; 173:1295–310. [PubMed: 18832567]
- Sonnino S, Prinetti A. Gangliosides as regulators of cell membrane organization and functions. *Adv Exp Med Biol*. 2010; 688:165–84. [PubMed: 20919654]
- Spravchikov N, Szyzakov G, Gartsbein M, Accili D, Tennenbaum T, Wertheimer E. Glucose effects on skin keratinocytes: implications for diabetes skin complications. *Diabetes*. 2001; 50:1627–35. [PubMed: 11423485]
- Stachelscheid H, Ibrahim H, Koch L, Schmitz A, Tschardt M, Wunderlich FT, et al. Epidermal insulin/IGF-1 signalling control interfollicular morphogenesis and proliferative potential through Rac activation. *Embo J*. 2008; 27:2091–101. [PubMed: 18650937]
- Suzuki K, Olah G, Modis K, Coletta C, Kulp G, Gero D, et al. Hydrogen sulfide replacement therapy protects the vascular endothelium in hyperglycemia by preserving mitochondrial function. *Proc Natl Acad Sci U S A*. 2011; 108:13829–34. [PubMed: 21808008]
- Tagami S, Inokuchi J, Kabayama K, Yoshimura H, Kitamura F, Uemura S, et al. Ganglioside GM3 participates in the pathological conditions of insulin resistance. *J Biol Chem*. 2002; 277:3085–92. [PubMed: 11707432]
- Terashi H, Izumi K, Deveci M, Rhodes LM, Marcelo CL. High glucose inhibits human epidermal keratinocyte proliferation for cellular studies on diabetes mellitus. *Int Wound J*. 2005; 2:298–304. [PubMed: 16618316]
- Usui ML, Mansbridge JN, Carter WG, Fujita M, Olerud JE. Keratinocyte migration, proliferation, and differentiation in chronic ulcers from patients with diabetes and normal wounds. *J Histochem Cytochem*. 2008; 56:687–96. [PubMed: 18413645]

- Wang X, Rahman Z, Sun P, Meuillet E, George D, Bremer EG, et al. Ganglioside modulates ligand binding to the epidermal growth factor receptor. *J Invest Dermatol.* 2001; 116:69–76. [PubMed: 11168800]
- Wang XQ, Sun P, Paller AS. Ganglioside induces caveolin-1 redistribution and interaction with the epidermal growth factor receptor. *J Biol Chem.* 2002; 277:47028–34. [PubMed: 12354760]
- Wang XQ, Sun P, Paller AS. Ganglioside GM3 inhibits matrix metalloproteinase-9 activation and disrupts its association with integrin. *J Biol Chem.* 2003; 278:25591–9. [PubMed: 12724312]
- Wang XQ, Yan Q, Sun P, Liu JW, Go L, McDaniel SM, et al. Suppression of epidermal growth factor receptor signaling by protein kinase C- α activation requires CD82, caveolin-1, and ganglioside. *Cancer Res.* 2007; 67:9986–95. [PubMed: 17942932]
- Wei D, Tao R, Zhang Y, White MF, Dong XC. Feedback regulation of hepatic gluconeogenesis through modulation of SHP/Nr0b2 gene expression by Sirt1 and FoxO1. *Am J Physiol Endocrinol Metab.* 2011; 300:E312–20. [PubMed: 21081708]
- Yamashita T, Hashiramoto A, Haluzik M, Mizukami H, Beck S, Norton A, et al. Enhanced insulin sensitivity in mice lacking ganglioside GM3. *Proc Natl Acad Sci U S A.* 2003; 100:3445–9. [PubMed: 12629211]
- Zador IZ, Deshmukh GD, Kunkel R, Johnson K, Radin NS, Shayman JA. A role for glycosphingolipid accumulation in the renal hypertrophy of streptozotocin-induced diabetes mellitus. *J Clin Invest.* 1993; 91:797–803. [PubMed: 8450061]
- Zhao H, Przybylska M, Wu IH, Zhang J, Maniatis P, Pacheco J, et al. Inhibiting glycosphingolipid synthesis ameliorates hepatic steatosis in obese mice. *Hepatology.* 2009; 50:85–93. [PubMed: 19444873]
- Zhao H, Przybylska M, Wu IH, Zhang J, Siegel C, Komarnitsky S, et al. Inhibiting glycosphingolipid synthesis improves glycemic control and insulin sensitivity in animal models of type 2 diabetes. *Diabetes.* 2007; 56:1210–8. [PubMed: 17470562]

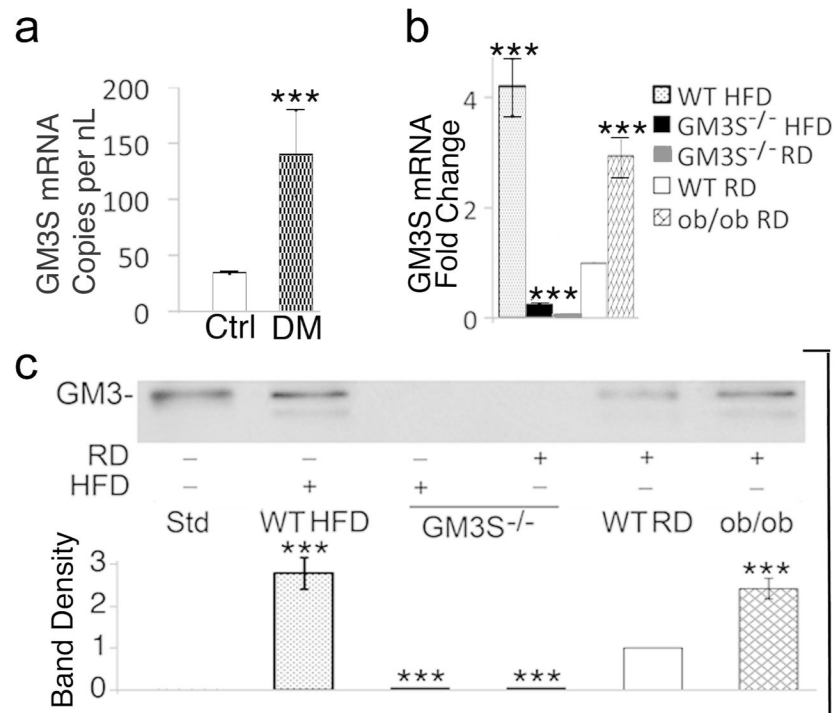


Figure 1. GM3 synthase and GM3 are increased in human and mouse diabetic skin

(a) Digital droplet PCR to measure GM3S expression in mRNA extracted from non-wounded human plantar skin (n=6 type 2 diabetics (DM) and n=5 age- and site-matched controls); mRNA is measured as copies per nL of PCR product. ***p<0.001; (b, c) Back skin was excised from DIO WT (HFD for 10 wks), ob/ob, GM3S^{-/-} (HFD; RD) and WT (RD) mice (n=5 in each group) for mRNA and glycosphingolipid extraction. qRT-PCR analysis (b) shows three runs in triplicate. Thin layer chromatography immunostaining with anti-GM3 antibody (c) is representative of 5 runs, shown densitometrically (Std = GM3 standard). Results are expressed as mean ± S.D. ***p<0.001, mouse DIO WT and ob/ob vs. WT RD or GM3S^{-/-}; GM3S^{-/-} mice vs. WT RD controls.

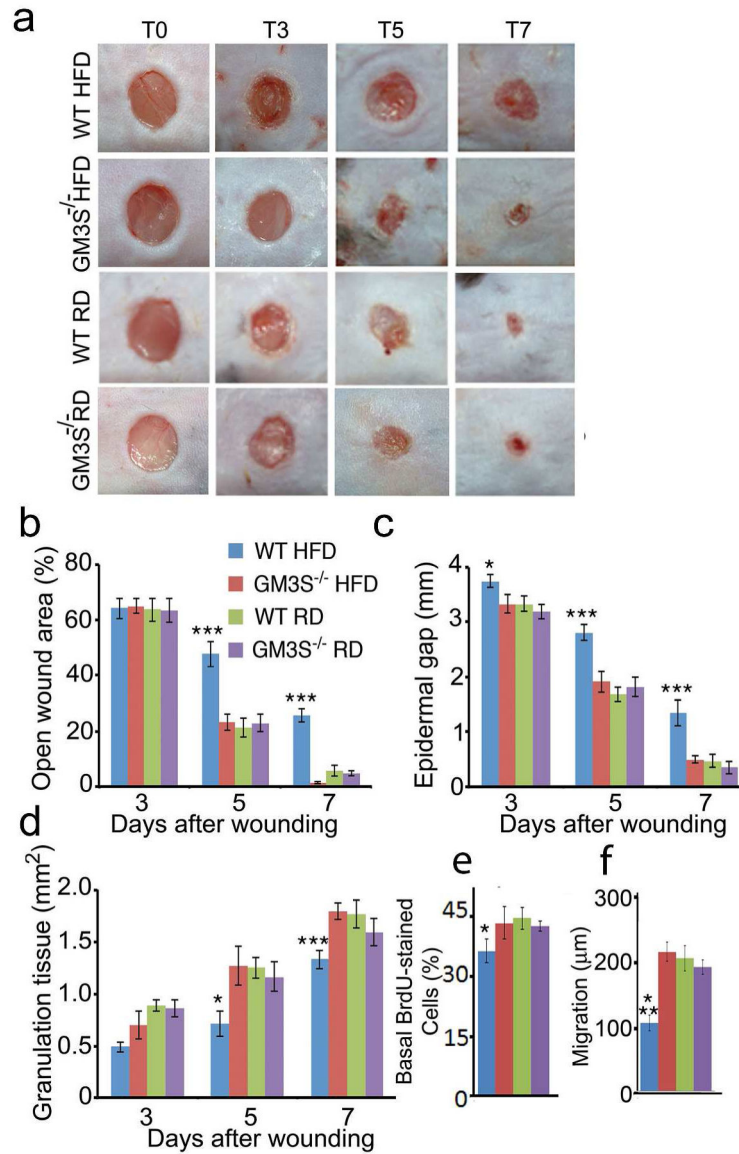


Figure 2. Ganglioside depletion accelerates wound healing in DIO mice

GM3S^{-/-} mice and wildtype (WT, GM3S^{+/+}) on a regular (RD) or high fat (HFD) diet for 10 wks. (a) Representative image of 20 wounds each group and time point. (b) Computerized measurements of open wound area. Epidermal gap (c) and granulation tissue area (d) measured by computerized morphometry. (e) *In vivo* proliferation as number of BrdU-positive basal keratinocytes. (f) Basal keratinocyte migration as epidermal length from wound edge to first BrdU-positive cell. At least 20 sections were analyzed for BrdU detection (3 day wounds) for each mouse group. Data shown are means \pm S.E. * $p < 0.05$, *** $p < 0.001$, for comparison of WT HFD vs. other mice and conditions, including GM3S^{-/-} HFD.

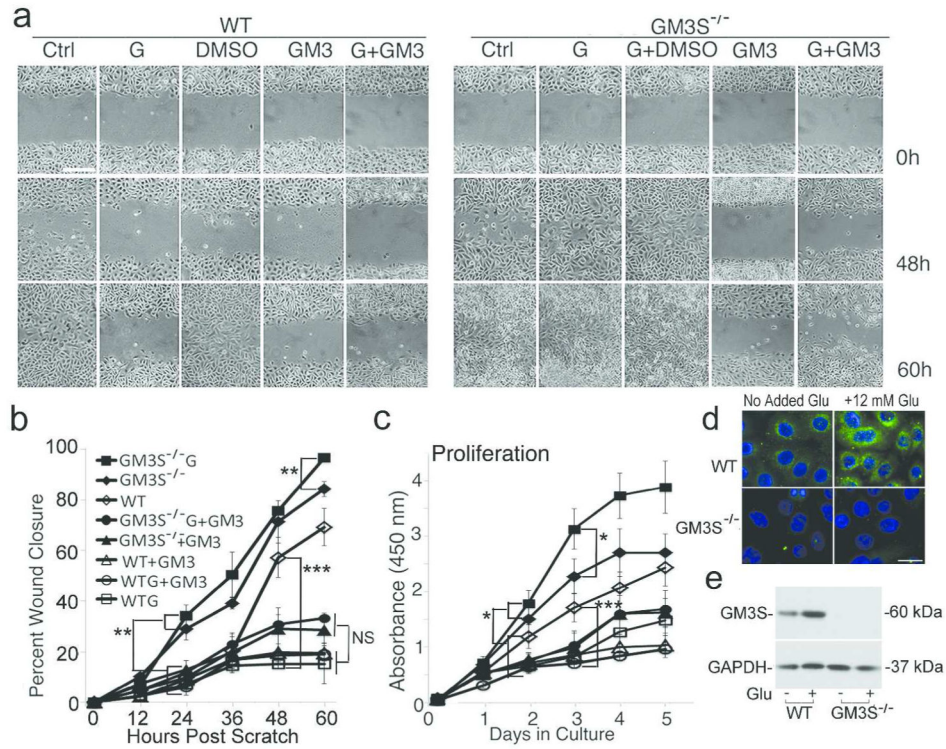


Figure 3. Ganglioside depletion prevents glucose-induced inhibition of proliferation and wound healing *in vitro*

(a) Migration of WT or GM3S^{-/-} KCs in standard or hyperglycemic (G) medium. Bar = 60 μ m. (b) Quantification of migration by computerized measurements of gap closure. **p<0.01, GM3S^{-/-} (\pm glucose (G)) vs. WT (\pm glucose or GM3) or GM3S^{-/-} + GM3 (\pm G) by 24h after scratch; ***p<0.001, WT vs. WTG, WT+GM3 (\pm G), and GM3S^{-/-}+GM3 (\pm G) by 48h; **p<0.01, GM3S^{-/-} G vs. GM3S^{-/-} by 60h. GM3S^{-/-}+GM3 (\pm G) cell closure did not differ from WTG (\pm GM3) at any time (at 60 h, p=0.06). NS = not significant. (c) Proliferation in standard, glucose-supplemented, or GM3-supplemented medium. *p<0.05, GM3S^{-/-} (\pm glucose) vs. WT (\pm glucose or GM3) by 2 d and GM3S^{-/-} G vs. GM3S^{-/-} by 3d; ***p<0.001, WT vs. WTG or WT + GM3 by 3d. (d) GM3 expression, as shown by immunofluorescence analysis and anti-GM3 antibody. Bar = 25 μ m. (e) Mouse KC GM3S protein as shown by Western immunoblotting with anti-GM3S antibody. Glu = 12 mM extra glucose. Assays performed 4 times in triplicate. Results expressed as mean \pm S.D.

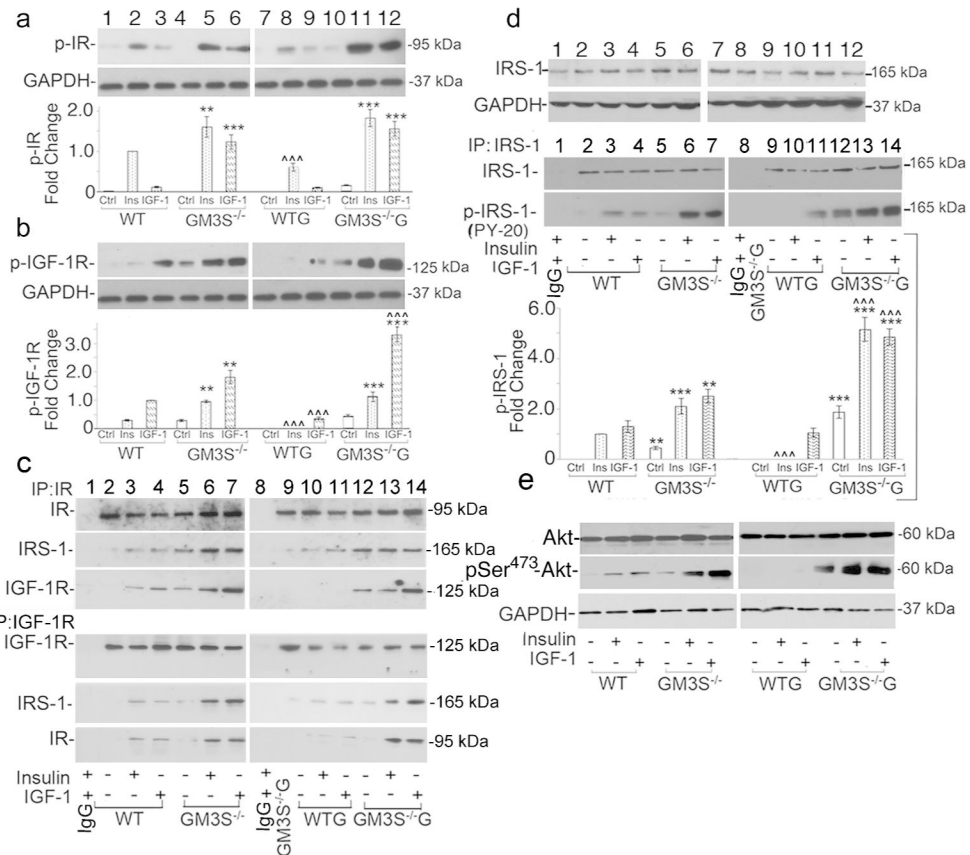


Figure 4. GM3 depletion activates IR/IGF-1R and downstream signaling

After starvation, KCs were treated with vehicle (Ctrl), insulin, or IGF-1 with (right) or without (left) supplemental glucose (G). Phosphorylation of IR (a) and IGF-1R (b) in whole cell lysates (top rows) was detected by p-IR and p-IGF-1R antibodies. (c) Association of immunoprecipitated IR and IGF-1R with IRS-1 (middle rows) and each other (bottom rows). First lane shows immunoprecipitation with IgG alone. (d) IRS-1 detected with anti-IRS-1 antibody (top row); phosphorylation of immunoprecipitated IRS-1 with PY-20 antibody (bottom row). First lane shows immunoprecipitation with IgG alone. Graph: results of 4 blots from 4 different experiments. (e) AKT (top) and p-AKT Ser⁴⁷³ (middle) and blots representative of 3 experiments. Blots in 4a–d are representative of 4 separate experiments; the blot in 4e of 3 separate experiments. Graphs for 4a, b, and d show data as quantified densitometrically and expressed as means±S.D. To be able to compare cells treated with and without excess glucose, all experiments were run in parallel. Results were normalized to GAPDH expression and then phosphorylation was expressed in comparison with WT KCs treated with the primary ligand of the receptor of interest (i.e., insulin for IR and IGF-1 for IGF-1R), which was assigned a fold change of 1. To show statistical significance, asterisks (*) compare GM3S^{-/-} vs. WT in all graphs with **p<0.01, ***p<0.001; carets (^) compare with vs. without supplemental glucose in all graphs for GM3S^{-/-} and WT KCs, ^^p<0.001.

